



**HAL**  
open science

## From toggle to precessional single laser pulse switching

Y. Peng, G. Malinowski, B. Kunyangyuen, D. Salomoni, J. Igarashi, J X Lin,  
W. Zhang, J. Gorchon, J. Hohlfeld, L D Buda-Prejbeanu, et al.

► **To cite this version:**

Y. Peng, G. Malinowski, B. Kunyangyuen, D. Salomoni, J. Igarashi, et al.. From toggle to precessional single laser pulse switching. *Applied Physics Letters*, 2024, 124 (2), pp.022405. 10.1063/5.0180359 . hal-04386592

**HAL Id: hal-04386592**

**<https://hal.science/hal-04386592>**

Submitted on 10 Jan 2024

**HAL** is a multi-disciplinary open access archive for the deposit and dissemination of scientific research documents, whether they are published or not. The documents may come from teaching and research institutions in France or abroad, or from public or private research centers.

L'archive ouverte pluridisciplinaire **HAL**, est destinée au dépôt et à la diffusion de documents scientifiques de niveau recherche, publiés ou non, émanant des établissements d'enseignement et de recherche français ou étrangers, des laboratoires publics ou privés.

This is the author's peer reviewed, accepted manuscript. However, the online version of record will be different from this version once it has been copyedited and typeset.

PLEASE CITE THIS ARTICLE AS DOI: 10.1063/1.50180359

1 **From toggle to precessional single laser pulse switching**

2

3 Y. Peng<sup>1</sup>, G. Malinowski<sup>1</sup>, B. Kuniyanguyen<sup>1</sup>, D. Salomoni<sup>2</sup>, J. Igarashi<sup>1</sup>, J. X. Lin<sup>1</sup>, W.  
4 Zhang<sup>1</sup>, J. Gorchon<sup>1</sup>, J. Hohlfeld<sup>1</sup>, L. D. Buda-Prejbeanu<sup>2</sup>, R. C. Sousa<sup>2</sup>, I. L. Prejbeanu<sup>2</sup>, D.  
5 Lacour<sup>1</sup>, S. Mangin<sup>1</sup> and M. Hehn<sup>1\*</sup>

6

7 <sup>1</sup> *Université de Lorraine, CNRS, IJL, F-54000 Nancy, France*

8 <sup>2</sup> *Univ Grenoble Alpes, , CEA, CNRS, Grenoble INP, SPINTEC, 38000 Grenoble, France*

9

10 \* *michel.hehn @univ-lorraine.fr*

11

12 **Keywords:**

13 Thin films, Rare Earth, Fast optics, Single pulse reversal, Spintronics

14

15

16

17 **Abstract**

18

19 With the advent of nanotechnologies, it has been possible to extend the number of stimuli that  
20 can be used to control the state of a magnetic nanostructure. Among those stimuli, single laser  
21 pulse excitation allows, under certain conditions, to obtain energy efficient ultra-fast  
22 magnetization reversal. With this respect, two different types of single pulse switching  
23 mechanisms have been reported. The first one consists in a sub picosecond ultrafast toggle  
24 switching which was observed mainly in Gd based alloys. The second type relies on sub-  
25 nanosecond precessional switching occurring in Rare Earth–Transition Metal  
26 alloys/multilayers. Here, we demonstrate that single pulse all optical switching is achieved in  
27  $\text{Co}_{68}\text{Tb}_{32}/\text{Co}_{100-x}\text{Gd}_x/\text{Co}_{68}\text{Tb}_{32}$  tri-layers in which the behavior can be tuned from toggle to  
28 precessional by changing the composition of the  $\text{Co}_{100-x}\text{Gd}_x$  alloy.

29

30

This is the author's peer reviewed, accepted manuscript. However, the online version of record will be different from this version once it has been copyedited and typeset.

PLEASE CITE THIS ARTICLE AS DOI: 10.1063/1.50180359

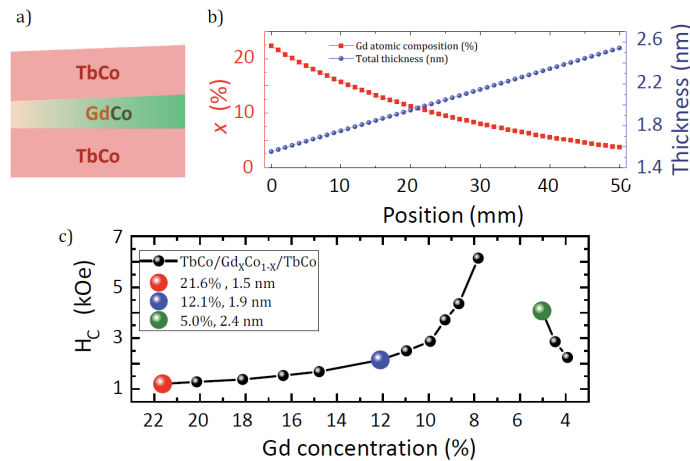
31 The challenge of controlling the magnetization at picosecond timescales in an energy efficient  
32 way is at the heart of future magnetic storage devices. With the advent of nanotechnologies, it  
33 has been possible to extend the number of stimuli that can be used to control the magnetic state  
34 of a magnetic material. In the form of thin films, multilayers or nanostructures, in a non-  
35 exhaustive list, the effects of strains, temperature gradients and spin-polarised currents are  
36 exasperated, allowing the magnetisation to be reversed without any applied magnetic field.  
37 On the other hand, the advent of femtosecond lasers has allowed the exploration of the  
38 magnetization dynamics on the ultrafast timescale<sup>1</sup>. Furthermore, it has been shown that, under  
39 certain conditions, ultrafast magnetization reversal can be achieved in a very energy-efficient  
40 process by the use of a single laser pulse<sup>2</sup>. Therefore, this research field area has caught the  
41 attention of a large part of the magnetism community. Those developments follow the major  
42 discovery of Bigot *et al.* in 1996 that a femtosecond laser pulse can demagnetize at a sub-  
43 picosecond time scale a Ni thin film<sup>1</sup>. Ten years later Stanciu *et al.* showed deterministic  
44 switching of a GdFeCo ferrimagnetic magnetic moment using a single circularly-polarized  
45 laser pulse<sup>2</sup> and later on, a toggle switching independent of the light helicity<sup>3,4</sup>. The current  
46 understanding is that the strong nonequilibrium electronic state and the transfer of angular  
47 momentum by exchange or spin current between antiferromagnetically exchanged coupled  
48 subnetworks are responsible for the toggle switching in Gd-based materials such as GdFeCo  
49 alloys<sup>4</sup>, Gd/Co multilayers<sup>5</sup> and GdTbCo<sup>6</sup>. The same arguments hold for Mn<sub>2</sub>Ru<sub>x</sub>Ga Heusler  
50 ferrimagnetic alloys which possess two inequivalent Mn sublattices and where ultrafast all-  
51 optical switching has been observed<sup>7</sup>. All other tests with rare earth alloys have failed so far.  
52 Interestingly, single pulse precessional switching has been shown in Tb/Co multilayer<sup>8,9,10</sup> and  
53 extended in a large variety of magnetic multilayers containing different rare earth (RE) (Tb,  
54 Dy) and transition metals (TM) (Co, Py and Fe) elements<sup>11</sup>. Taking advantage of ultrafast heat  
55 transfer to the lattice in RE-TM alloys, the in-plane reorientation of the magnetization of the  
56 multilayer launches a precessional reversal. In this process, the reversal threshold is  
57 independent of the pulse duration for pulse duration lower than 10ps. Here, we demonstrate  
58 that single pulse switching is achieved in Co<sub>68</sub>Tb<sub>32</sub>/Co<sub>100-x</sub>Gd<sub>x</sub>/Co<sub>68</sub>Tb<sub>32</sub> tri-layers whose  
59 behavior can be tuned from toggle to precessional by changing the Co<sub>100-x</sub>Gd<sub>x</sub> concentration.

60  
61 The multilayers were grown by sputtering in an AJA system with a base pressure less than  
62  $5 \times 10^{-8}$  mbar to ensure oxygen free deposition of RE materials. The sample is made of  
63 Glass/Ta(5 nm)/Pt(5 nm)/Co<sub>68</sub>Tb<sub>32</sub>(4 nm)/Co<sub>100-x</sub>Gd<sub>x</sub>(t)/Co<sub>68</sub>Tb<sub>32</sub>(4 nm)/Ta(5 nm)/Pt(1 nm) as  
64 shown in figure 1(a). The Ta/Pt buffer and capping layers ensure adhesion of the substrate and  
65 protection against oxidation. The alloys are made by co-deposition of different sources  
66 arranged in a confocal geometry, the composition being adjusted by the powers applied on the  
67 different guns. For all layers, except for the Co<sub>100-x</sub>Gd<sub>x</sub>(t) layer, the homogeneity of the layer is  
68 obtained by rotating the sample. The Co<sub>100-x</sub>Gd<sub>x</sub>(t) is obtained by co sputtering of Co and Gd  
69 pure targets. Composition/thickness wedge is obtained by stopping the rotation of the sample  
70 during deposition. Since Co and Gd are mounted diametrically opposed, a natural gradient of  
71 concentration is obtained. Since the deposition rate of Co and Gd are not identical, a gradient  
72 of thickness also exists. A calibration of the position dependent deposition rate has been done<sup>11</sup>.  
73 The local thickness and composition could be calculated. The values are reported in figure 1(b).  
74 In full films, Co<sub>100-x</sub>Gd<sub>x</sub> is known to have its compensation around  $x = 20\%$ <sup>12,13</sup>. One must be  
75 aware that the Co<sub>100-x</sub>Gd<sub>x</sub> interfaces can affect the compensation composition as it was shown  
76 in ref [14] especially in the case of thin layers. For thicknesses less than 4 nm, it was shown  
77 that Co<sub>100-x</sub>Gd<sub>x</sub> can have a perpendicular to the film plane magnetic anisotropy (PMA)<sup>15</sup>.  
78 In the multilayer, the Co<sub>68</sub>Tb<sub>32</sub>(4 nm) are kept constant. Considering the concentration,  
79 Co<sub>68</sub>Tb<sub>32</sub> is Tb dominant. Due to the high RE content, the alloy has a Curie temperature roughly  
80 373 K above room temperature<sup>12</sup> and possesses PMA.

This is the author's peer reviewed, accepted manuscript. However, the online version of record will be different from this version once it has been copyedited and typeset.

PLEASE CITE THIS ARTICLE AS DOI: 10.1063/5.0180359

81



82

83

84

85

86

87

88

89

90

91

92

93

94

95

96

97

98

99

100

101

102

103

104

105

106

107

108

109

110

**Figure 1.** (a) Schematic of the trilayer stack; (b) Variation of the thickness (blue) and Gd composition (red) as a function of position in the wedge sample; (c) Variation of coercive field,  $H_c$ , versus Gd composition. Red, blue and green dots correspond to the composition of the samples whose reversal is shown in figure 2.

In  $\text{Co}_{68}\text{Tb}_{32}(4 \text{ nm})/\text{Co}_{100-x}\text{Gd}_x(t)/\text{Co}_{68}\text{Tb}_{32}(4 \text{ nm})$ , the Co atoms are strongly ferromagnetically exchange coupled at the interface. Therefore, Tb and Gd magnetization subnetwork are parallel. We performed Kerr magnetometer hysteresis loops in the polar geometry to check PMA, coercivity and subnetwork dominance. As can be seen in figure 1(c), a divergence of the coercive field associated with the change of subnetwork dominance is the sign of the net magnetisation compensation of the  $\text{Co}_{68}\text{Tb}_{32}(4 \text{ nm})/\text{Co}_{100-x}\text{Gd}_x(t)/\text{Co}_{68}\text{Tb}_{32}(4 \text{ nm})$  trilayer. It appears with  $x$  around 6 to 7 % confirming the Tb dominance in the  $\text{Co}_{68}\text{Tb}_{32}$  alloy (more Co in  $\text{Co}_{100-x}\text{Gd}_x$  is needed to get the total compensation). In all cases, PMA could be observed.

For the single shot reversal experiments, a Ti:sapphire femtosecond-laser source was used with a wavelength of 800 nm and a 5 kHz repetition rate for the pump-probe experiments. LED light probe source with a wavelength of 628 nm was used to obtain MOKE images. Since samples have been grown on glass substrate, pump laser excitation was done on the glass side of the sample while MOKE microscope observation was done on the layers side. Details on the sample growth, on MOKE microscope and pump-probe setups can be found in [11].

Single pulse magnetization switching experiments have been done for concentration range  $x$  from 5 to 22 % and measurements performed for  $x = 5 \%$ , 12.1 % and 21.6 % are reported in figure 2a. When  $x = 21.6 \%$ , a perfect single shot switching is observed. On the other hand, when  $x = 5 \%$ , single-shot switching was observed along with the stabilization of a ring structure. In between, a multi-domain state occurs as seen for  $x = 12.1 \%$ . A more detailed study of reversal mechanism is obtained by measuring state diagrams that report the static magnetic state as a function of both pulse duration and fluence as shown in figure 2 b and c.

This is the author's peer reviewed, accepted manuscript. However, the online version of record will be different from this version once it has been copyedited and typeset.

PLEASE CITE THIS ARTICLE AS DOI: 10.1063/1.50180359

111  
112  
113  
114  
115  
116  
117  
118  
119  
120  
121  
122  
123  
124  
125  
126  
127  
128  
129  
130  
131  
132  
133  
134  
135  
136  
137  
138  
139

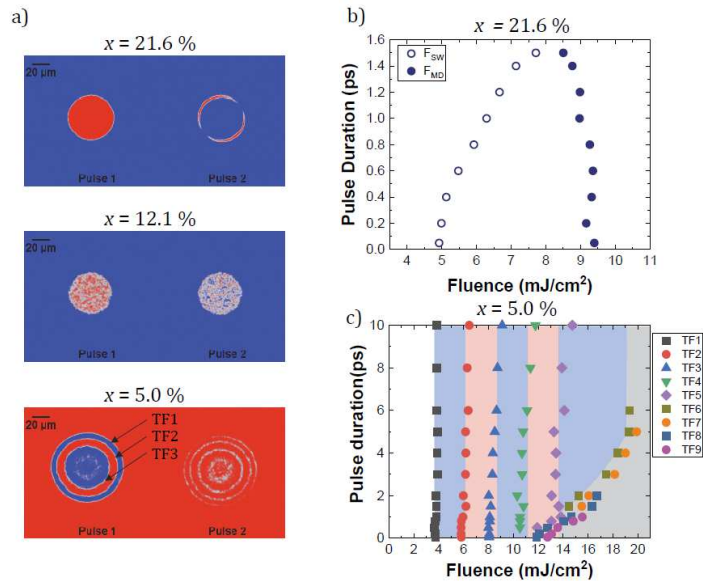


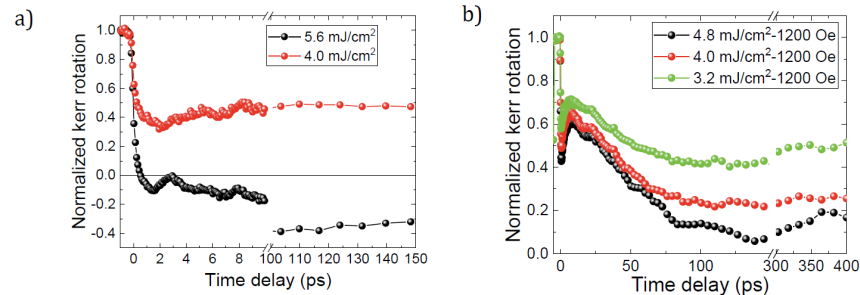
**Figure 2.** (a) Single pulse reversal experiments done for the samples with 21.6 % (5.9  $\text{mJ}/\text{cm}^2$ ), 12.1 % (10.3  $\text{mJ}/\text{cm}^2$ ) and 5 % (10.3  $\text{mJ}/\text{cm}^2$ ) Gd contents, identified in red, blue and green in figure 1c. Pulse duration versus fluence state diagram measured for 21.6 % of Gd (b) and 5 % of Gd (c). In b)  $F_{\text{SW}}$  and  $F_{\text{MD}}$  correspond to the fluence to get single shot switching or multidomain state respectively. In c) the complex domain pattern require the definition of multiple threshold fluence : TF1 corresponds to the appearance of outer blue ring and can be referred as  $F_{\text{SW}}$  for the ring structure, TF2 to the appearance of the red ring etc...TF9 corresponds to  $F_{\text{MD}}$ .

The state diagrams differ strongly when  $x = 21.6\%$  and  $x = 5\%$ . As far as the state diagram of  $x = 21.6\%$  is concerned (figure 2b), two fluence thresholds can be defined :  $F_{\text{SW}}$  and  $F_{\text{MD}}$  that correspond to the fluence needed to induce the switching and a multidomain state respectively. The triangular shape of this state diagram is characteristic of toggle reversal in Gd-based materials<sup>16</sup>. Since  $F_{\text{SW}}$  depends on pulse duration, the underlying mechanism is likely governed by the electronic temperature which decreases with increasing the pulse duration as discussed in [16,17]. On the other hand, since  $F_{\text{MD}}$  depends only slightly on pulse duration, a link to the Curie temperature, the energy transferred to the lattice and so the stabilisation of multi-domain structure is highly probable as suggested in [17,18,19]. As far as the state diagram of  $x = 5\%$  is concerned, the domain pattern is much more complex and multiple threshold fluence have to be defined  $TF_n$ <sup>11</sup> : TF1 corresponds to the appearance of outer blue ring and can be referred as  $F_{\text{SW}}$  for the ring structure, TF2 to the appearance of the red ring etc... The fact that the critical fluences (TF1, TF2,...) are mostly independent of pulse duration implies an underlying mechanism linked to the energy transferred to the lattice<sup>11</sup>. A careful analysis of the position of the boundaries that separates the rings has shown that they are always located at the same local threshold energy<sup>11</sup>, independently of surrounding domains and/or local in-plane heat gradients.

This is the author's peer reviewed, accepted manuscript. However, the online version of record will be different from this version once it has been copyedited and typeset.

PLEASE CITE THIS ARTICLE AS DOI: 10.1063/1.50180359

140 More insight in the reversal process is gained by the analysis of the pump-probe measurements.  
 141 Results are reported in figure 3. For the sample with  $x = 21.6\%$ , dynamics of reversal has been  
 142 measured for two fluences :  $F = 4.0 \text{ mJ/cm}^2$  and  $F = 5.6 \text{ mJ/cm}^2$  that corresponds to fluences  
 143 for which reversal does not occur and occurs respectively when pulse duration is fixed to 50 fs  
 144 (see figure 2b). We can clearly see in figure 3a that typical demagnetization occurs and  
 145 magnetization crosses zero at 600 fs. Full reversal occurs at 40 ps before magnetization  
 146 recovers at longer time scale because of applied field to reset the magnetization for the pump  
 147 probe experiments. As far as the sample with  $x = 5\%$  is concerned, the measurements show  
 148 that after a fast demagnetization at a time scale of some 100 fs, the magnetization first recover,  
 149 similarly to the conventional demagnetization/re-magnetization shown in various  
 150 ferromagnetic and ferrimagnetic materials. At longer timescales, a few tens of picoseconds, a  
 151 magnetization decrease is observed. This decrease is attributed to the reorientation of the  
 152 magnetization in the plane of the layers<sup>11</sup>. The existence of the DC field, in combination to a  
 153 strongly damped reorientation of the anisotropy, makes the precession difficult to be  
 154 observed<sup>11</sup>.  
 155



156  
 157 **Figure 3.** Pump-probe dynamics measured for 21.6 % of Gd (a) and 5 % of Gd (b) at different  
 158 fluences. The pulse duration has been fixed to 50 fs.  
 159  
 160

161 A summary of the different fluence threshold measured as a function of Gd content and for a  
 162 pulse duration fixed to 50 fs is reported in figure 4.  
 163

164 We can clearly see that for  $x$  above 12.5 %, the  $\text{Co}_{68}\text{Tb}_{32}(4 \text{ nm})/\text{Co}_x\text{Gd}_{100-x}(\text{t})/\text{Co}_{68}\text{Tb}_{32}(4 \text{ nm})$   
 165 trilayer behaves like Gd based materials presenting single shot ultrafast toggle switching: 1)  
 166  $F_{\text{sw}}$  increases as the Gd content decreases within the range of 22 % to 16 %. The deterministic  
 167 switching of the CoGd alloy is conditioned by the amount of spin current generated through  
 168 the demagnetization of the Gd subnetwork. The increase of  $F_{\text{sw}}$  indicates that the  
 169 demagnetization of Gd needs to be increased to keep a significant spin current since its  
 170 concentration is decreased. 2) Conversely, as the magnetic compensation point occurs around  
 171  $x = 20\%$  [12,13], the saturation magnetization of CoGd (and demagnetizing fields) increases  
 172 as the Gd content decreases from 16 % to 12 %. This increase in saturation magnetization,  
 173 coupled with a decrease in anisotropy, results in an overall reduction in effective anisotropy,  
 174 promoting the formation of magnetic domains. These changes in the 16-to-12 % range lead to  
 175 a reduction of the critical threshold for multi-domain formation.  
 176

177 In the 8-to-12.5 % range,  $F_{\text{MD}}$  becomes smaller than  $F_{\text{sw}}$ , and therefore only a final  
 178 multidomain state is observed. Interestingly, in this range of composition, a close analysis of

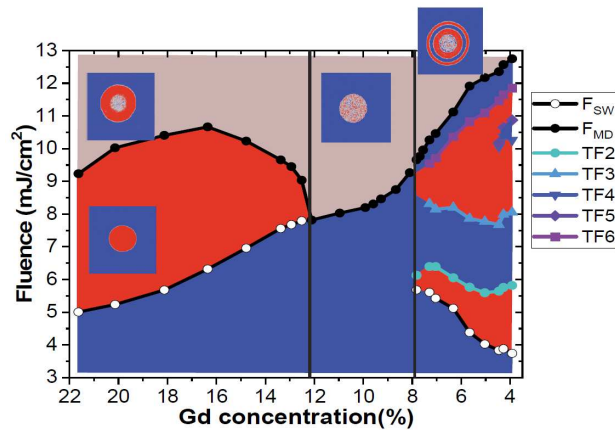
This is the author's peer reviewed, accepted manuscript. However, the online version of record will be different from this version once it has been copyedited and typeset.

PLEASE CITE THIS ARTICLE AS DOI: 10.1063/1.50180359

179 the magneto-optical signal (figure 2a, 12.1 %) reveals that a fraction of the magnetization  
 180 toggles after each laser shot, even though the majority of the exposed area appears  
 181 demagnetized. Possibly, a transient reversal might be still taking place in the 8-to-12.5 % range,  
 182 which is then hindered or erased by the demagnetizing fields that promote multi-domain  
 183 formation.

184  
 185 Finally, when  $x$  is less than 8 %, the  $\text{Co}_{68}\text{Tb}_{32}(4\text{ nm})/\text{Co}_x\text{Gd}_{100-x}(t)/\text{Co}_{68}\text{Tb}_{32}(4\text{ nm})$  undergoes  
 186 a precessional reversal with the appearance of multiple threshold fluences<sup>11</sup>. As can be seen in  
 187 figure 4, it occurs even for rather low fluences (down to 3.5  $\text{mJ}/\text{cm}^2$ ). This behaviour is  
 188 observed when the  $\text{Co}_x\text{Gd}_{100-x}$  layer undergoes an in-plane reorientation that launches the  
 189 precession of magnetization<sup>11</sup>. Finally, we believe that another key ingredient for the reversal  
 190 around this composition range is the rather low overall saturation magnetization (and  
 191 demagnetizing fields) of the stacks which increases the multi-domain threshold and stabilizes  
 192 large domains.

193  
 194 In order to cover the composition range from 4 % et 22 % of Gd, in the geometry of our AJA  
 195 PVD system, different deposition rates have to be used for Gd and Co. This leads unfortunately  
 196 also to a wedge in thickness. We know from our previous work that the thickness of the TM  
 197 layer in RE-TM alloy/TM/RE-TM alloy trilayers has an impact on the precessional reversal  
 198 [11]. Therefore, we tested if the thickness  $t$  of  $\text{Co}_x\text{Gd}_{100-x}(t)$ , with  $t$  around the thickness of  
 199  $\text{Co}_{95}\text{Gd}_5(2.6\text{ nm})$ , has an impact on the reversal in the 20 % to 10 % composition range. We  
 200 found that the toggle switching is kept for  $t$  up to 3.5 nm. Only the size of the reversed domain  
 201 and the composition to get into demagnetized state slightly change. So, we undoubtedly  
 202 demonstrate that the concentration  $x$  is the most important parameter to consider in this study.  
 203  
 204



205  
 206 **Figure 4.** Threshold fluences as a function of Gd concentration for a pulse duration fixed to 50  
 207 fs. The colors correspond to the magnetic state starting from a saturated blue state. At low  
 208 fluences, the state is not modified. At high fluence, the pink area denotes a demagnetized state.  
 209 In between, the behavior depends on gadolinium concentration.  
 210

211 In conclusion, we demonstrate that single pulse all optical switching is achieved in  
 212  $\text{Co}_{68}\text{Tb}_{32}/\text{Co}_{100-x}\text{Gd}_x/\text{Co}_{68}\text{Tb}_{32}$  tri-layers in which the behavior can be tuned from toggle to



This is the author's peer reviewed, accepted manuscript. However, the online version of record will be different from this version once it has been copyedited and typeset.

PLEASE CITE THIS ARTICLE AS DOI: 10.1063/5.0180359

213 precessional by changing the composition of the  $\text{Co}_{100-x}\text{Gd}_x$  alloy. In order to promote toggle  
 214 switching,  $\text{Co}_{100-x}\text{Gd}_x$  alloy needs to keep PMA. Furthermore, the spin current coming from the  
 215 demagnetization of Gd has to be large enough and remains the key ingredient to promote the  
 216 toggle switching. This behavior stands till a multidomain state is observed which is a sign that  
 217  $F_{\text{SW}} > F_{\text{MD}}$ . On the other hand, precessional switching occurs for low Gd concentration. In this  
 218 case, the spin current generated by the Gd demagnetization is strongly decreased while the net  
 219 magnetization increases and so does the demagnetization field, favoring the in-plane  
 220 reorientation of the magnetization. This work emphasize the role of magnetic anisotropy on the  
 221 laser induced ultrafast magnetization reversal in complex magnetic multilayers which is  
 222 foreseen as a candidate for magneto-photonic memory applications.  
 223

#### 224 References

- 225 1. Beaupaire, E., Merle, J.-C., Daunois, A. & Bigot, J.-Y. Ultrafast spin dynamics in  
 226 ferromagnetic nickel. *Phys. Rev. Lett.* 76, 4250 (1996).  
 227 2. Stanciu, C. D., Hansteen, F., Kimel, A. V., Kirilyuk, A., Tsukamoto, A., Itoh, A. & Rasing,  
 228 Th. All-Optical Magnetic Recording with Circularly Polarized Light. *Phys. Rev. Lett.* 99,  
 229 047601 (2007).  
 230 3. Radu, I., Vahaplar, K., Stamm, C., Kachel, T., Pontius, N., Durr, H. A., Ostler, T. A., Barker,  
 231 J., Evans, R. F. L., Chantrell, R. W., Tsukamoto, A., Itoh, A., Kirilyuk, A., Rasing, T. & Kimel,  
 232 A. V. Transient ferromagnetic-like state mediating ultrafast reversal of antiferromagnetically  
 233 coupled spins. *Nature* 472, 205-209 (2011).  
 234 4. Ostler, T. A., Barker, J., Evans, R. F. L., Chantrell, R. W., Atxitia, U., Chubykalo-Fesenko,  
 235 O., El Moussaoui, S., Le Guyader, L., Mengotti, E., Heyderman, L. J., Nolting, F., Tsukamoto,  
 236 A., Itoh, A., Afanasiev, D., Ivanov, B. A., Kalashnikova, A. M., Vahaplar, K., Mentink, J.,  
 237 Kirilyuk, A. & Kimel, A. V. Ultrafast heating as a sufficient stimulus for magnetization reversal  
 238 in a ferrimagnet. *Nature Communications* 3, 666 (2012).  
 239 5. Lalieu, M. L., Peeters, M. J. G., Haenen, S. R. R., Lavrijsen, R. & Koopmans, B.  
 240 Deterministic all-optical switching of synthetic ferrimagnets using single femtosecond laser  
 241 pulses. *Phys. Rev. B* 96, 220411 (2017).  
 242 6. Zhang, W., Lin, J. X., Huang, T. X., Malinowski, G., Hehn, M., Xu, Y., Mangin, S. &  
 243 Zhao, W. Role of spin-lattice coupling in ultrafast demagnetization and all optical helicity-  
 244 independent single-shot switching in  $\text{Gd}_{1-x}\text{Tb}_y\text{Co}_x$  alloys. *Phys. Rev. B* 105, 054410  
 245 (2022).  
 246 7. Banerjee, C., Teichert, N., Siewierska, K. E., Gercsi, Z., P. Atcheson, G. Y., Stamenov, P.,  
 247 Rode, K., Coey, J. M. D. & Besbas, J. Single pulse all-optical toggle switching of  
 248 magnetization without gadolinium in the ferrimagnet  $\text{Mn}_2\text{Ru}_x\text{Ga}$ . *Nature Communications* 11,  
 249 4444 (2020).  
 250 8. Avilés-Félix, L., Álvaro-Gómez, L., Li, G., Davies, C. S., Olivier, A., Rubio-Roy, M.,  
 251 Auffret, S., Kirilyuk, A., Kimel, A. V., Rasing, T., Buda-Prejbeanu, L. D., Sousa, R. C., Dieny,  
 252 B. & Prejbeanu, I. L. Integration of Tb/Co multilayers within optically switchable  
 253 perpendicular magnetic tunnel junctions. *AIP Advances* 9, 125328 (2019).  
 254 9. Avilés-Félix, L., Olivier, A., Li, G., Davies, C. S., Álvaro-Gómez, L., Rubio-Roy, M.,  
 255 Auffret, S., Kirilyuk, A., Kimel, A. V., Rasing, T., Buda-Prejbeanu, L. D., Sousa, R. C., Dieny,  
 256 B. & Prejbeanu, I. L. Single-shot all-optical switching of magnetization in Tb/Co multilayer-  
 257 based electrodes. *Scientific Reports* 10, 5211 (2020).  
 258 10. Mishra, K., Blank, T. G. H., Davies, C. S., Avilés-Félix, L., Salomoni, D., Buda-Prejbeanu,  
 259 L. D., Sousa, R. C., Prejbeanu, I. L., Koopmans, B., Rasing, Th., Kimel, A. V. & Kirilyuk, A.  
 260 Dynamics of all-optical single-shot switching of magnetization in Tb/Co multilayers, *Phys.*  
 261 *Rev. Research* 5, 023163 (2023).



This is the author's peer reviewed, accepted manuscript. However, the online version of record will be different from this version once it has been copyedited and typeset.

PLEASE CITE THIS ARTICLE AS DOI: 10.1063/5.0180359

- 262 11. Y. Peng, D. Salomoni, G. Malinowski, W. Zhang, J. Hohlfeld, L. D. Buda-Prejbeanu, J.  
 263 Gorchon, M. Vergès, J. X. Lin, R.C. Sousa, I. L. Prejbeanu, S. Mangin and M. Hehn. In plane  
 264 reorientation induced single laser pulse magnetization reversal. *Nature Communication* (2023).  
 265 <https://doi.org/10.1038/s41467-023-40721-z>  
 266 12. Hansen, P., Clausen, C., Much, G., Rosenkranz, M. & Witter, K. Magnetic and magneto -  
 267 optical properties of rare - earth transition - metal alloys containing Gd, Tb, Fe, Co. *J. Appl.*  
 268 *Phys.* 66, 756 (1989).  
 269 13. Lin, J.-X., Hehn, M., Hauet, T., Peng, Y., Igarashi, J., Le Guen, Y., Remy, G., Gorchon, J.,  
 270 Malinowski, G., Mangin, S., Hohlfeld, J., Single laser pulse induced magnetization switching  
 271 in in-plane magnetized GdCo alloys. <http://arxiv.org/abs/2308.10516>  
 272 14. Bello, J.-L., Lacour, D., Migot, S., Ghanbaja, J., Mangin, S., Hehn, M., Impact of interfaces  
 273 on magnetic properties of Gdx(Fe90Co10)1-x alloy, *Appl. Phys. Lett.* 121, 212402 (2022); doi:  
 274 10.1063/5.0125011.  
 275 15. Guo, Z., Wang, J., Malinowski, G., Zhang, B., Zhang, W., Wang, H., Liu, C., Peng, Y.,  
 276 Vallobra, P., Xu, Y., Jenkins, S., Chantrell, R. W., Evans, R. F. L., Mangin, S., Zhao, W., Hehn,  
 277 M., Single-shot laser-induced switching of an exchange biased antiferromagnet,  
 278 arXiv:2302.04510  
 279 16. Wei, J.; Zhang, B.; Hehn, M., Zhang, W., Malinowski, G., Xu, Y., Zhao, W. and Mangin,  
 280 S., All-optical Helicity-Independent Switching State Diagram in Gd-Fe-Co Alloys, *Phys. Rev.*  
 281 *Applied* 15, 054065 (2021).  
 282 17. Gorchon, J., Wilson, R. B., Yang, Y., Pattabi, A., Chen, J. Y., He, L., Wang, J. P., Li, M.  
 283 and Bokor, J., Role of electron and phonon temperatures in the helicity-independent all-  
 284 optical switching of GdFeCo, *Phys. Rev. B* 94, 184406 (2016).  
 285 18. Zhang, W., Hohlfeld, J., Huang, T. X., Lin, J. X., Hehn, M., Le Guen, Y., Malinowski,  
 286 G., Zhao, W. S., Mangin, S., Criteria to observe a single-shot all optical switching in Gd-  
 287 based ferrimagnetic alloys, under preparation (2023).  
 288 19. Verges, M., Zhang, W., Remy, Q., Le-Guen, Y., Gorchon, J., Malinowski, G., Mangin, S.,  
 289 Hehn, M., Hohlfeld, J., Extending the scope and understanding of all-optical magnetization  
 290 switching in Gd-based alloys by controlling the underlying temperature transients, submitted  
 291 to *Phys. Rev. Lett.* (2023).

292  
 293 **Acknowledgements**

294 We also acknowledge financial support from the ANR (ANR-17-CE24-0007 UFO project), the  
 295 Region Grand Est through its FRFCR call (NanoTeraHertz and RaNGE projects), by the impact  
 296 project LUE-N4S part of the French PIA project "Lorraine Université d'Excellence", reference  
 297 ANR-15IDEX-04-LUE and by the "FEDER-FSE Lorraine et Massif Vosges 2014-2020", a  
 298 European Union Program. D.S. has received funding from the European Union's Horizon 2020  
 299 research and innovation programme under Marie Skłodowska-Curie grant agreement No  
 300 861300 (COMRAD).